CERN/MPS/OP 74-4
10 May 1974

# EFFICIENCIES OF INTERNAL DUMP TARGETS IN THE CPS

D.M. Lewis and Ch. Steinbach

## ABSTRACT

This report discusses the mathematical methods used to determine the efficiency of beam dumping by internal dump targets. The calculation is performed by a simulation program run on the CDC 7600, and the results, obtained for various dump targets, are presented. Finally a recommendation is made for the design of the new internal dump target for the PS.

## 1. INTRODUCTION

The operation of the CPS with high intensity beams from the PSB has attracted a great deal of attention to the problem of beam dumping[1-7]. One method of destroying the beam is to move a metal block into the path of the beam, i.e. an internal beam dump target. This report describes the calculation of dumping efficiency by this method and includes proposals for the parameters of the head of the dump target.

The dumping efficiency is defined here as the percentage number of protons which encounter nuclear interaction and scattering events inside the block, as in Hereward et al.[8]; these protons are then assumed lost in the close vicinity of the dump, while the remainder are allowed to circulate in the machine until either lost on the chamber wall or intercepted by the dump on subsequent machine revolutions. Three methods of beam intervention have been considered:

i) a horizontally-moving block from inside the machine and accelerated outwards at around 0.75g, thus increasing the number of protons striking the dump due to energy losses from previous dump traversals;

ii) a vertically-falling block, being the simplest to design mechanically;

iii) a guillotine-shaped block, facing outwards from the machine and falling under gravity; this combines the advantages of the two previous types.

Efficiency calculations were performed, assuming the PS to be operating on its "flat top" during dumping. In fact all protons are lost soon after the first traversal of the dump and the results would be practically the same had the accelerating part of the cycle been studied.

## 2. METHOD OF CALCULATION

Dumping efficiencies are estimated by a Monte Carlo simulation calculation. The criteria for assessing beam behaviour are described in this section.

### 2.1 Simulation of beam shape in transverse phase space

The spatial coordinates of each proton are given by the betatron oscillationn ($\alpha$) and the phase angle ($\phi$) in each transverse plane; since the beam shape is essentially Gaussian[9] the distribution function for betatron amplitudes takes the form:

$$P(\alpha) = K_1 \alpha \exp\left[-\alpha^2/2\sigma^2\right] , \qquad (1)$$

where $\sigma^2$ is the variance of the projected beam in real space, and values for $\sigma$ may be obtained from Brouzet et al.[10,11]. Here one is forced to take a realistic upper limit for $\alpha$, namely $A_{max}$, so that

$$P'(\alpha) = K_2 P(\alpha) , \qquad (2)$$

and normalization is performed by integration from $\alpha = 0$ to $\alpha = A_{max}$. A random choice of betatron amplitude may be obtained by equating the random number R (where $0 \leq R \leq 1$) to

$$R = S(\alpha) = \int_0^\alpha P'(x)\,dx \,. \tag{3}$$

In practice, it is more efficient to rearrange this function

$$G(R) \equiv S^{-1}(\alpha) \,, \tag{4}$$

so that for each random number R, one has a betatron amplitude associated with it and

$$\left.\begin{aligned} G(0) &= 0 \\ G(1) &= A_{max} \end{aligned}\right\} \tag{5}$$

Hence for any random number R, linear interpolation between stored values of G will give

$$\alpha = \frac{(R - r_n) \times \left[G(r_{n+1}) - G(r_n)\right]}{h} + G(r_n) \,, \tag{6}$$

where R is the random number given

$h = (N - 1)^{-1}$, where N is the number of stored values of function G,

$r_n$ = (integer value of R divided by R) × h,

$r_{n+1} = r_n + h$.

This method is carried out independently in the vertical and horizontal planes, for each proton; the actual spatial coordinates are determined as follows:

i) For a horizontal dump: the horizontal coordinate is taken at its minimum point (i.e. $\cos\phi = -1$ or $x = -\alpha_x$) and the vertical phase angle chosen randomly.

ii) For a vertical dump: the horizontal phase angle is chosen randomly and the vertical coordinate is taken at the maximum of the betatron oscillation (i.e. $\cos\phi = 1$ or $z = +\alpha_z$).

iii) For a guillotine-type dump: the proton is considered to be at the extremities of its betatron motion in both planes, namely:

$$\cos\phi_x = -1$$

$$\cos\phi_z = +1 \,.$$

Finally longitudinal momentum is chosen from a Gaussian distribution about an equilibrium momentum:

$$A(p) = \frac{1}{\sqrt{2\pi\sigma_p^2}} \exp\left\{\frac{-(p - p_0)^2}{2\sigma_p^2}\right\}, \tag{7}$$

where $\sigma_p$ is an experimentally known parameter[12].

2.2 Nuclear scattering

The probability that a proton will have encountered a nuclear interaction or scattering event on traversing an absorber block of length L is

$$P(L) = 1 - \exp(-n\sigma_{tot}L) , \tag{8}$$

where n is the atomic number density ($cm^{-3}$),

$\sigma_{tot}$ is the total proton-nuclear scattering cross-section.

Values of $\sigma_{tot}$ were obtained from Bellettini et al.[13] and Barashenkov et al.[14]. The criterion for determining whether absorption (nuclear scattering) has occurred is to check whether $\ell \leq L$, where

$$\ell = \frac{\ln\left[1/(1 - R)\right]}{n\sigma_{tot}} \tag{9}$$

and R is again a random number.

2.3 Coulomb scattering

The cumulative effect of many small atomic scattering events is to produce a finite deflection on the proton trajectory. The deflection θ is taken as normally distributed according to the Rossi theory[15] with a variance of

$$\sigma_s^2 = \left(\frac{E_s}{pc\beta}\right)^2 \frac{L}{X_{rad}} , \tag{10}$$

where $E_s$ ≡ 15 MeV for transversely projected angles,

p = momentum in GeV/c,

L = length of material traversed,

$X_{rad}$ = the radiation length for the material.

The scattered angles then take the values

$$\left.\begin{aligned} \theta_x &= R_1\sigma_s \\ \theta_z &= R_2\sigma_s \end{aligned}\right\} \tag{11}$$

where $R_1$, $R_2$ are normally distributed random numbers with unit variance.

## 2.4 Ionization energy losses

Protons traversing the dump also lose energy to the surrounding medium, which is considered as a reduction in its longitudinal momentum. This energy loss is (from Ref. 15):

$$\frac{dE}{dx} = - 4\pi r_0^2 \, mc^2 N \left[ \ln \frac{2mc^2}{I} - \ln (1 - \beta^2) - 1 \right] , \qquad (12)$$

where E, m, c are the fundamental constants in c.g.s.,

$r_0$ is the first Bohr radius,

N is the mean electron density [in $cm^{-3}$],

I is the mean excitational energy of the atom, in electron volts[16],

$\beta = v/c$.

Values of energy losses for the more relevant metals are given in Fig. 1. This energy loss produces a shift of the equilibrium orbit towards the centre machine by

$$\Delta r = \alpha R \frac{\Delta p}{p} , \qquad (13)$$

where R is the radius of the machine,

$\alpha$ is the momentum compaction factor at the location of the dump.

## 2.5 Motion around the machine

Protons circulating in the machine are considered to follow pure betatron oscillations about an equilibrium orbit. The frequencies determined by the values of Qr and Qv used: the variation of Qr with radius being accounted for [values given in Brouzet[17] and Azzoni[18]]. The effect of closed-orbit deviations is allowed for, by specifying three values for maximum deviations; namely, $x_1$, $x_2$, $z_1$ and then reducing the effective aperture of the chamber to

$-(73.0 + x_1)$ to $(73.0 - x_2)$ mm horizontally

and

$\pm (35.0 - z_2)$ mm vertically.

A proton is assumed lost on the chamber wall whenever one of its betatron amplitudes (determined in real or mm units) exceed one of these limits. This, however, does assume that the maximum of oscillation occurs in the same region as the maximum closed orbit deviation and so overestimates the effect. Rather than construct an exact model for the machine, which would vary considerably under different operating conditions, it is more meaningful to choose "most probable" values for $x_1$, $x_2$, and $z_1$.

The situation is further complicated by the fact that the equilibrium orbit for a proton shifts after every dump traversal and the shift depends on whether the dump is located in an F or D section; this so-called "wriggle" must be accounted for.

## 2.6 Proton scattering out of the dump

Protons striking the dump near its edge will have a finite probability of being scattered out of the dump before traversing the full dump length; hence the position, where a proton strikes the front face of the dump, becomes important. Since both Qr and Qv are close to 6.25, it can be assumed that prior to impact, the proton was nearest the dump, four machine revolutions earlier (this is correct for the three types of dumps). So, in the case of a dump moving horizontally the criteria for dump impact is

$$x = \alpha \cos \phi = - \alpha \ , \tag{14}$$

while four machine revolutions earlier

$$x' = \alpha \cos (\phi - 8\pi Qr) \ , \tag{15}$$

and so

$$\Delta x_1 = 32\pi^2 (\Delta Q)^2 \alpha \ , \tag{16}$$

where $Qr = 6.25 + \Delta Q$.

Also, during this period of four machine revolutions, the dump is accelerating towards the centre of the chamber and so, for the horizontal case, travels a distance

$$\Delta x_2 = 4\tau [2acc\ (73 - \alpha)]^{\frac{1}{2}} \ , \tag{17}$$

where $\tau$ is the period for one machine revolution,
acc is the propelled acceleration of the dump target.

The exact point of impact is chosen randomly over a length of $(\Delta x_1 + \Delta x_2)$; typical values give $\Delta x_1$ and $\Delta x_2$ orders of magnitude of 0.1 and 0.01 mm, respectively. It is then necessary to reconstruct the proton path through the dump, given that the deflection in any one transverse direction is

$$\Delta y = \frac{2\theta_1}{3} \sqrt{\ell^3/L} + \theta_0 \ell \ , \tag{18}$$

where $\theta_1$ is the total Coulomb scattering angle,
$\theta_0$ is the initial angle of impact,
L is the total dump length,
$\ell$ is the longitudinal length traversed at any point.

It an "outscattering" event has occurred, the traversal length may be calculated from Eq. (18), the energy loss reduced proportionately, the probability of absorption reduced and if relevant the final Coulomb scattered angles reduced by:

$$\theta_i = \theta_1 \sqrt{\ell_i/L} \ , \tag{19}$$

### 2.7 Misalignment of the dump

In practice, it is virtually impossible to ensure perfect alignment of the dump target with the axis of the vacuum chamber and this misalignment influences the efficiency of the system, since the edge of the dump now acts as a scatterer.

### 2.8 Beam scraping

To reduce the effect of "outscattering", it is possible to mount a beam scraper on the edge of the dump. The added angular deflection increases the betatron amplitude, so that on some subsequent machine revolution the proton will strike the dump at a larger distance from the edge; then the probability of "outscattering" is very small, e.g. a 2 mm thick copper scraper will provide a jump of around 5 mm for 24 GeV/c protons in an F section. This effect is discussed in the next section.

## 3. RESULTS OF CALCULATIONS

Each estimate of dumping efficiency is based on an initial sample of $10^4$ protons and incurs standard errors of between 0.2 and 0.5% on the estimate itself. Unless otherwise stated, the beam emittances horizontally and vertically are taken as $2\pi$ and $1\pi$ mm·mrad as given by Barbalat[19]; this is considered a stable beam at 24 GeV/c. The closed-orbit parameters are set to ±10 mm horizontally and zero vertically, in accordance with the algorithm described in Section 2.5.

### 3.1 The length of the dump

Estimates of the vertical efficiency as a function of dump length are given in Fig. 2, for the four metals -- aluminium, iron, copper and tungsten; the proton mean energy being 24.0 GeV. As expected, light materials are more efficient for short dump lengths, whereas for longer dumps heavy metals are more favourable. This comes from the fact that for short targets the process is essentially multi-traversal and that low scattering and energy loss avoid losses on the vacuum chamber during the revolutions between two traversals. For long targets, the average number of traversals decreases towards one and a short interaction length is the main parameter to give good efficiencies.

Finally the best choice, for medium lengths around 15 cm, is copper.

### 3.2 Mode of beam intervention

The efficiency estimates for the three types of dump (horizontal, vertical and guillotine) were compared at several dump lengths, but it was not possible to establish any one type as being the most efficient. This was the case at the longer dump lengths, where the statistical errors in the estimates became quite small. Increasing the protons samples above $10^4$ so as to elucidate this point was considered extravagant computing due to the obviously small improvement in efficiency to be gained ($\lesssim 0.3\%$).

### 3.3 Energy variation

The above calculations for vertical dumps were extended to a range of initial proton energies 10-28 GeV and the variations in efficiency for typical absorber blocks are given in Fig. 3. In the actual calculation the tacit assumption is made that the PS is operating on its "flat top", but the data given here can still be considered accurate for beam stopping during acceleration. This is due to the fact that the average number of machine revolutions before total proton loss is very small and in fact this figure is smaller for low proton energies.

### 3.4 Dumping efficiency for different beam conditions

The estimates were found to be quite insensitive to the shape of the beam; again the calculations were performed for vertical dumps at 24 GeV, see Fig. 4. A range of initial emittances were tested 2-12π mm·mrad, horizontally, and 1-6π mm·mrad, vertically. However, variation of closed-orbit parameters gave significant reductions in efficiency for dumps shorter than 30 cm. As expected, only small changes in these parameters are required, especially for the inner horizontal component, since some 85% of the protons lost onto the chamber walls are in fact lost in this direction. The "ideal" dump efficiencies of Section 3.7 could be reduced by at least 5% for a relatively minor change in closed orbit.

### 3.5 Effect of the misalignment

The graph of Fig. 5 shows the results to be expected for misalignment of a 15 cm copper dump struck by 24 GeV protons. The shape of the curve suggests that a scatterer would improve the dumping efficiency, the physical explanation being that, for small angles, the increased penetration on the front surface of the dump after scattering lowers the probability of outscattering on subsequent traversals.

### 3.6 The effect of beam scrapers

The criterion for efficient beam scraping is that:

$$\left(\frac{x_\ell}{X_{rad_1}}\right)^{\frac{1}{2}} >> x_b \frac{E}{E_s\beta} + \frac{1}{\beta}\left(\frac{x_d}{X_{rad_2}}\right)^{\frac{1}{2}} , \qquad (20)$$

where $x_\ell$, $x_b$ are the thickness and protrusion length of the scraper,

$\beta$ is the betatron amplitude function in mm units for the appropriate direction and location of the momentum jump,

$x_d$ is the beam stopper length,

$E$ is the proton energy in GeV,

$E_s$ is the Rossi energy constant in MeV, see Eq. (10).

It was shown that protrusion lengths of 1 mm were sufficient for scraping. Figure 6 shows the efficiency as a function of scraper thickness for several different lengths of copper, the proton energy again at 24 GeV thus demonstrating that scraping does enhance the dumping efficiency for blocks above 10 cm lengths.

### 3.7 The location of the dump

Slight improvements in efficiency can be obtained by locating:

a) a horizontally-moving dump in an F section,

b) a vertically-moving dump in a D section,

the differences being no greater than 5% for a 5 cm length of copper, cf. Fig. 7, and are unimportant for lengths of 15 cm and above.

## 4. CONCLUSION

After due consideration of the above information, we propose that an internal dump target should be constructed with the following physical parameters:

i) copper dump of around 15 cm length, covering the whole aperture of the vacuum chamber;

ii) due to the simpler mechanical construction, a vertically-moving dump, preferably located in a D section (though an F section is not considerably worse);

iii) a copper scraper mounted on the front wall of the block with the dimensions of 2 mm × 1 mm, will improve the efficiency and also distribute the heat losses.

Acknowledgements

The authors would like to thank L. Henny for reading through this report.

Distribution: As requested.

## REFERENCES


1) O. Barbalat, Décharge du faisceau PS -- essai de synthèse du séminaire du PS du 14 mars 1972, MPS/DL Note 73-3.

2) Machine and Areas Committee, Summary of meeting No. 11 (13 August, 1973), MPS/DL/Min 73-20.

3) D. Dekkers, Décharge du faisceau PS; discipline générale concernant l'emploi d'un faisceau de haute intensité, MPS/CO Note 73-65.

4) Ch. Steinbach and J.P. Potier, Dumping the high intensity beam, MPS/CO Note 71-27.

5) Ch. Steinbach, Possibility of vertical dumping in a fixed block in the CPS, MPS/CO Note 73-2.

6) R. Gouiran, A possibility for internal beam dumping in the CPS; the movable dump solution, MPS/SR/Note 73-7.

7) Ch. Steinbach, Resonant internal dumping, MPS/OP Note 74-5.

8) H.G. Hereward, J. Ranft and W. Richter, Efficiency of multi-traversal targets, CERN 65-1 (1965).

9) C. Bovet, C.D. Johnson and K.O. Pedersen, Computerized treatment of ionization beam scanner signals, 8th Int. Conf. on High-Energy Accelerators, CERN, Geneva, September 1971, p. 450.

10) E. Brouzet, C. Johnson et P. Lefèvre, Mesures des dimensions verticales du faisceau du PS, MPS/DL Note 70-21.

11) E. Brouzet, Mesures des dimensions du faisceau interne PS à moyenne et haute enérgie, MPS/Int. CO 68-21.

12) O. Barbalat, CPS beam emittances, MPS/DL Note 71/16.

13) G. Bellettini et al., Nuclear Phys. 79, 609 (1966).

14) V.S. Barashenkov et al., Energy dependence of the nuclear cross-sections for nucleons at energies above 50 MeV, Dubna preprint P2-4183.

15) E. Segré, Experimental nuclear physics, Vol. I, Chapter II, p. 168.

16) W.H. Barkas and M.J. Berger, Tables of energy losses and ranges of heavy charged particles, NAS-NRC Publication 1133/Part 7.

17) E. Brouzet, Reglage du courant PFW à haute energie, MPS/Int. CO 68-27.

18) G. Azzoni, Mesure de Qr and Qv à differentes energies, MPS/CO Note 72-25.

19) O. Barbalat, Beam emittance estimates, MPS/DL Note 72-42.

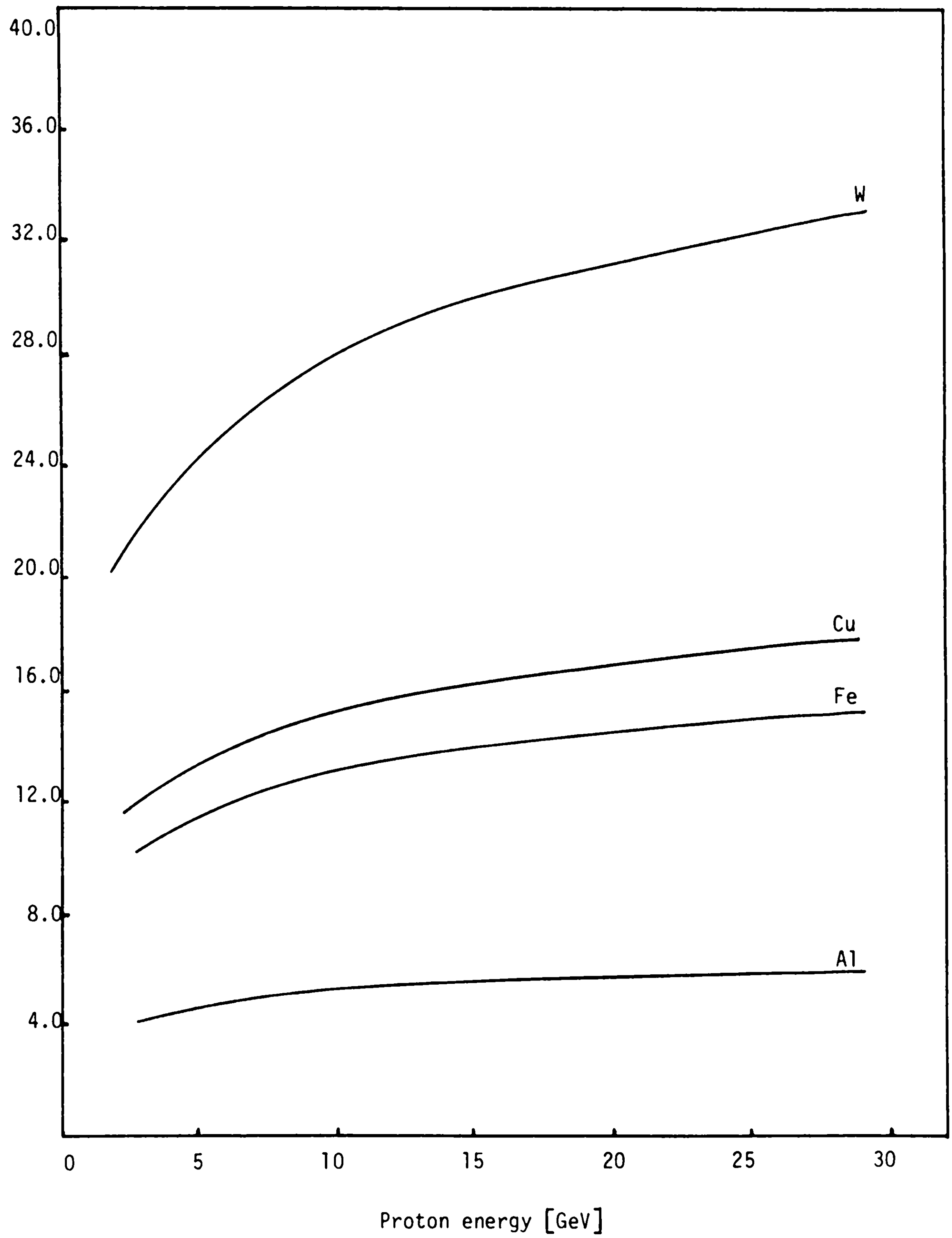


Fig. 1 : Ionization losses in metals [units: $MeV \cdot cm^{-1}$].

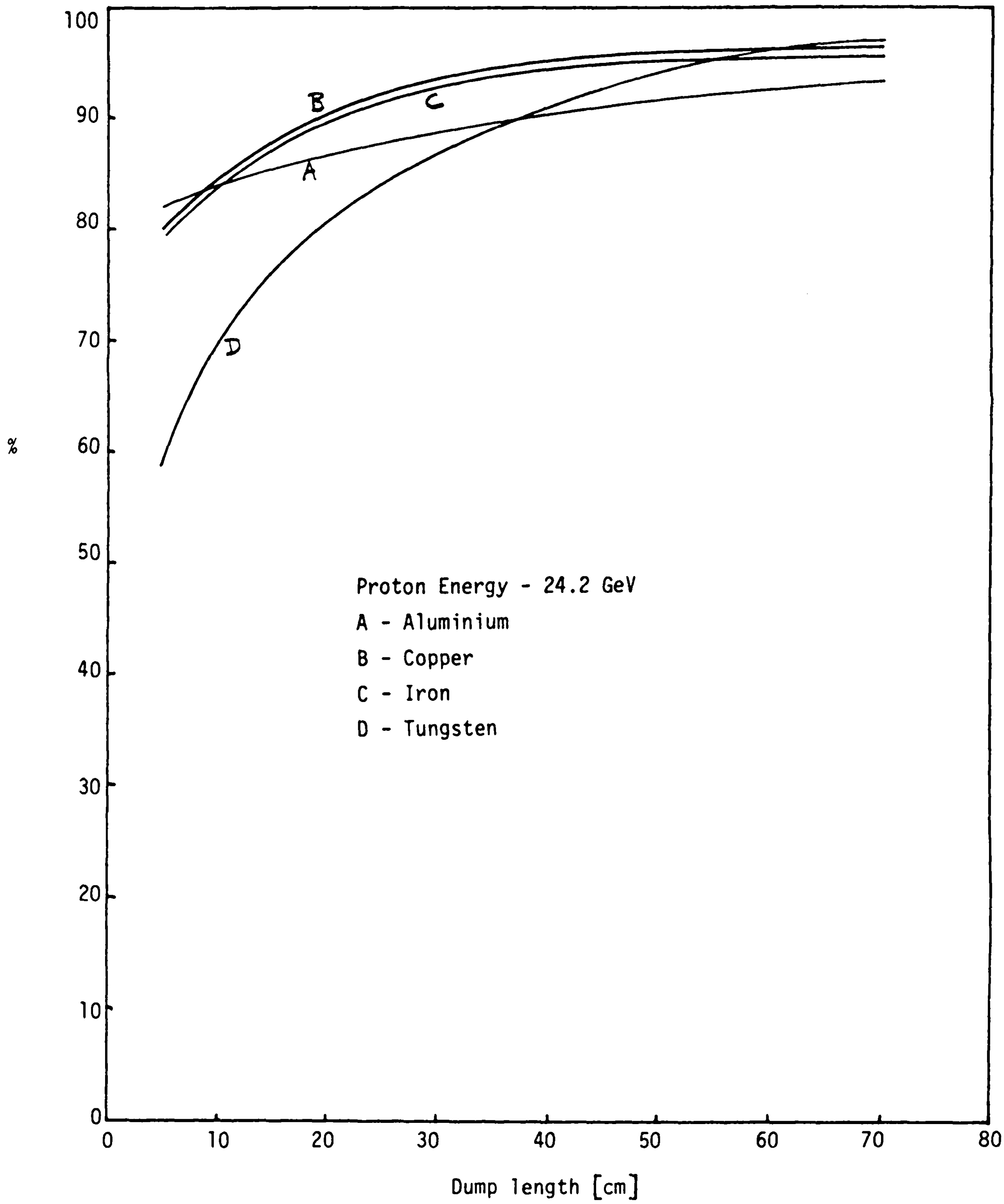


Fig. 2 : Efficiency versus dump length.

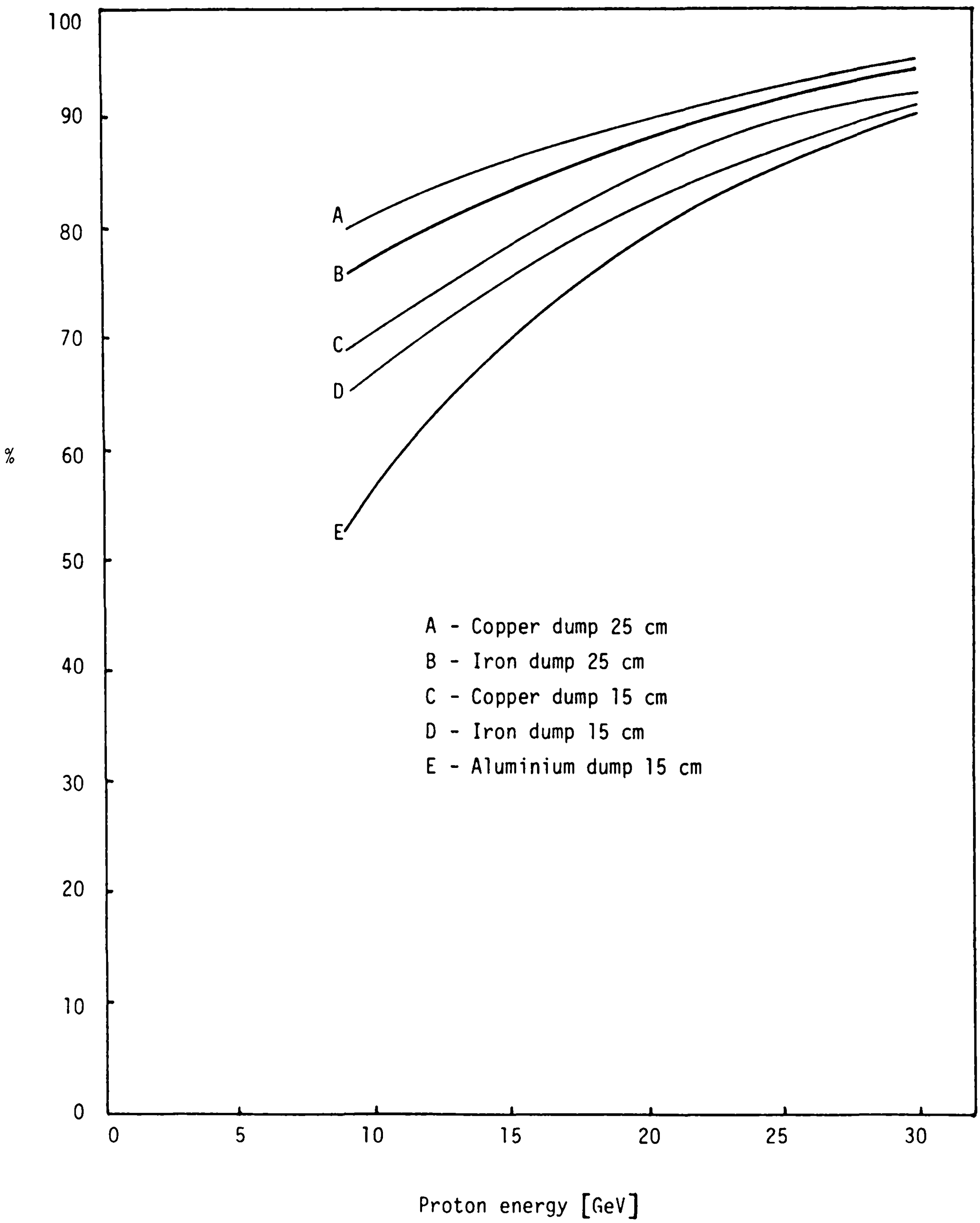


Fig. 3 : Dump efficiency versus proton energy.

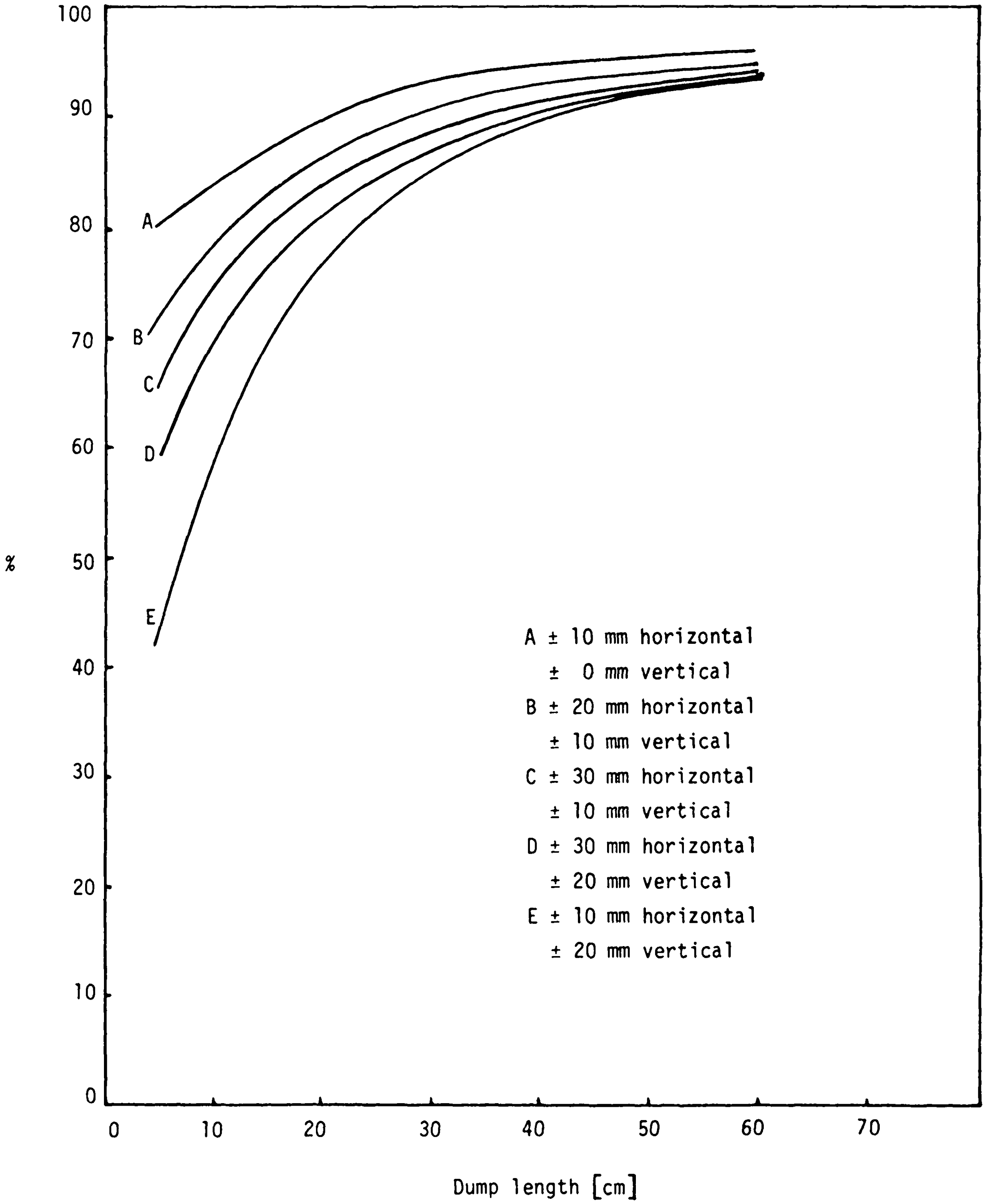


Fig. 4 : Efficiency versus dump length for various ~~closed-orbit~~ beam size parameters.

15 cm Cu target (vertical)

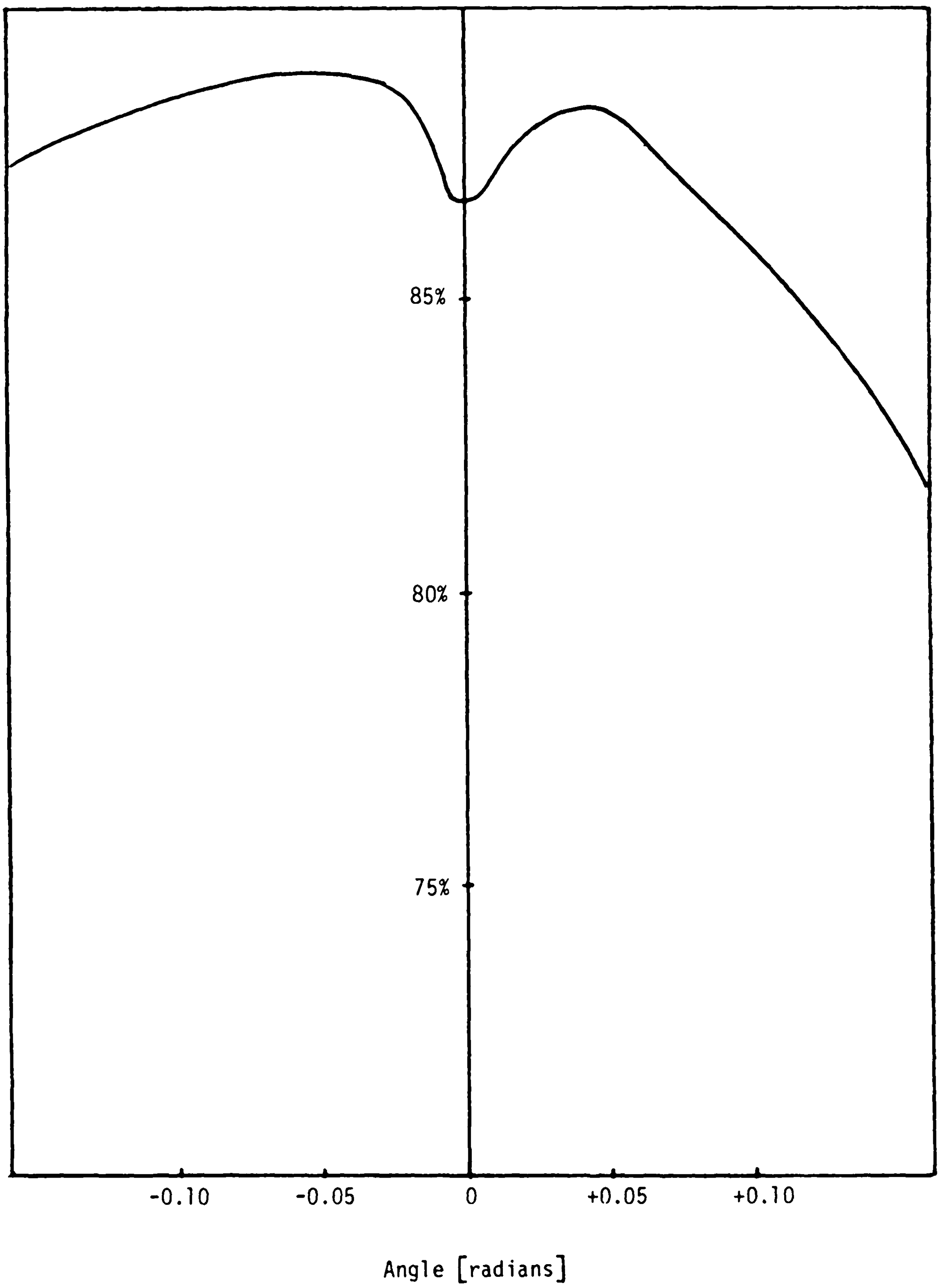


Fig. 5 : Efficiency versus angle of "tilt" for 15 cm copper dump target at 24 GeV.

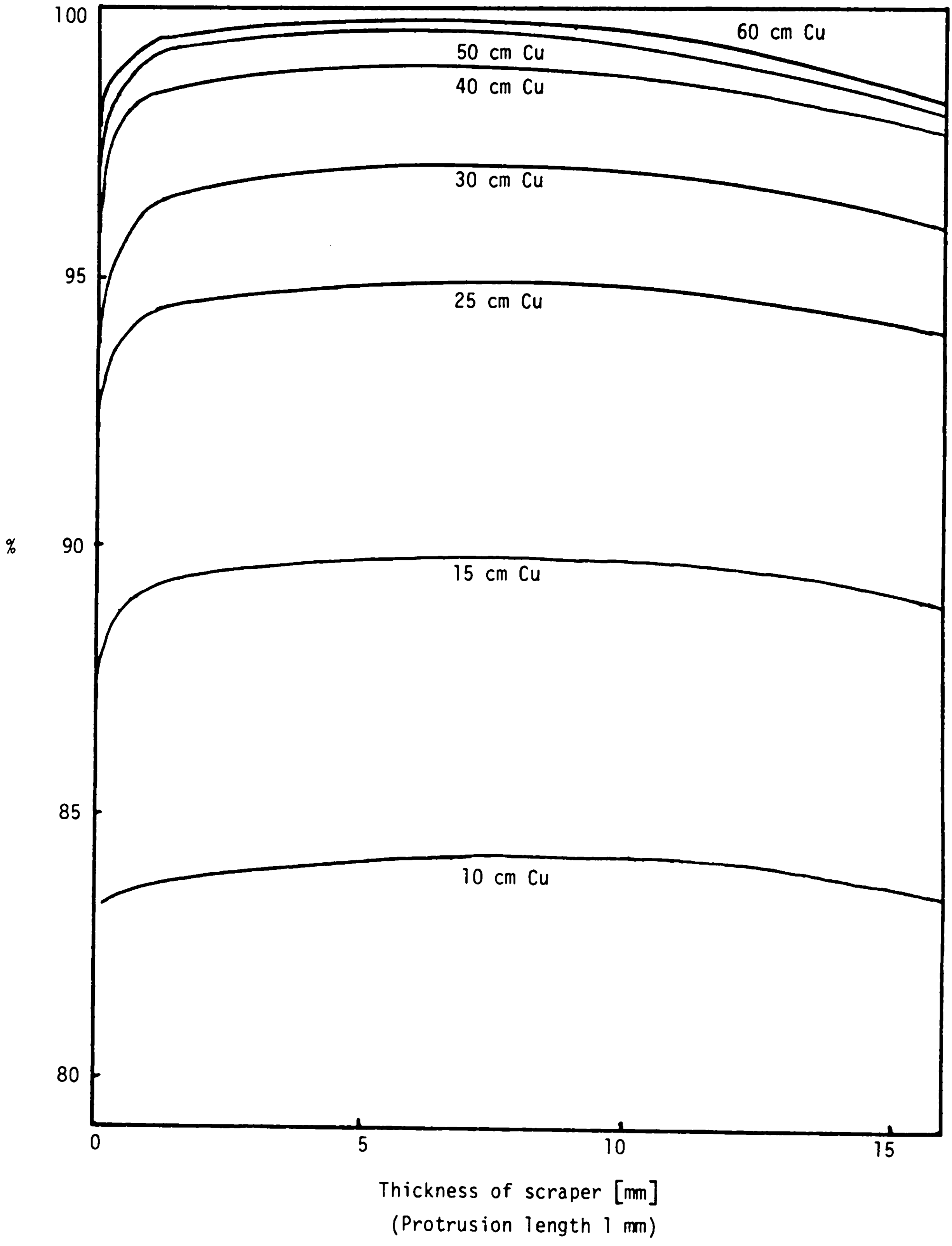


Fig. 6 : Efficiency versus dump length for different scraper thicknesses.

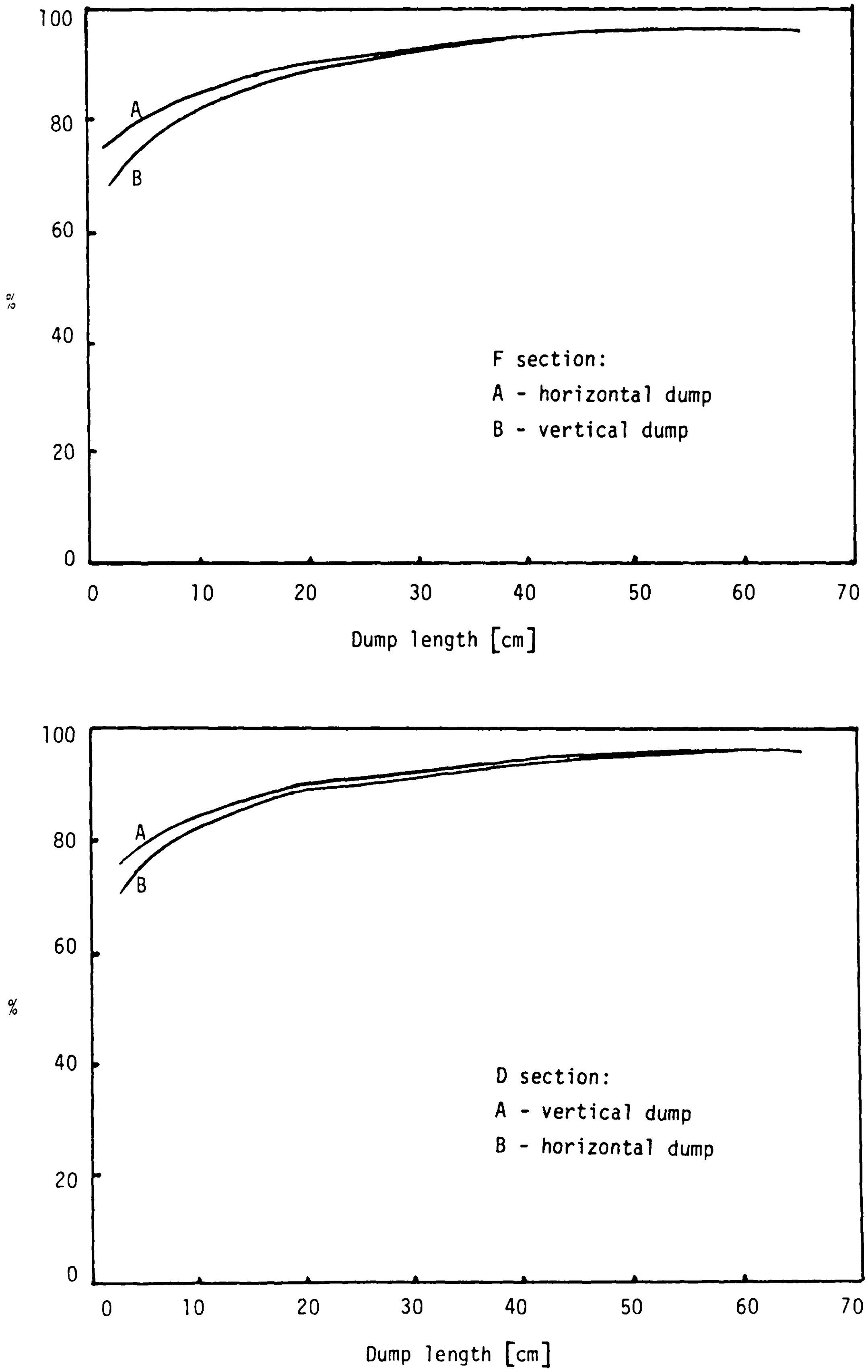


Fig. 7 : Efficiency versus dump length (Cu)